Available online at www.sciencedirect.com
ScienceDirect
Polyhedron 26 (2007) 2276–2280
POLYHEDRON
www.elsevier.com/locate/poly

A family of ferrocene-rich Mn_7, Mn_8 and Mn_{13} clusters

Antonio Masello, Muralee Murugesu, Khalil A. Abboud, George Christou *

Department of Chemistry, University of Florida, Gainesville, FL 32611-7200, USA

Received 21 October 2006; accepted 13 November 2006
Available online 18 November 2006

Abstract

The use of ferrocene-1,1′-dicarboxylic acid ($fdcH_2$) in Mn cluster chemistry has led to a family of ferrocene-rich Mn_7, Mn_8 and Mn_{13} clusters. The complexes are all mixed-valence. Solid-state DC and AC magnetic susceptibility studies have established the Mn_7, Mn_8 and Mn_{13} complexes to possess $S = 2$, 5 and 9/2 ground states, respectively.

Keywords: Manganese; Clusters; Crystal structures; Mixed valence; 1,1′-Ferrocenedicarboxylate

Transition metal clusters continue to attract great interest within the inorganic chemistry and related disciplines primarily because of their interesting and often unusual magnetic properties. Such clusters are also interesting for other reasons and potential applications in materials science and catalysis [1]. One of the most important aspects of clusters containing paramagnetic metal ions is their behavior as single-molecule magnets (SMMs), which offers potential applications as nanoscale magnetic materials [2]. For these reasons, our group has a longstanding interest in developing new synthetic routes to high nuclearity transition metal clusters, and we have usually employed carboxylate ligation, either alone or in combination with other ligand types. A large number of products have been obtained from these efforts, many of them new examples of SMMs.

As part of a new direction initiated recently, we have sought to expand the functionality of these complexes by introducing ligands that are able to easily undergo reversible redox processes. The idea is that this could provide a useful means of altering the electron count of the system, and thus allow a study of the effect of this on the magnetic properties of the molecule. The ligand we chose was ferrocene-1,1′-dicarboxylate (fdc^{2-}), which has been used only once previously in Mn chemistry [3]. The ferrocene unit allows for fast and reversible one-electron processes, which accounts for the extensive prior development of ferrocene-based chemistry. There are thus many examples in the literature of ferrocene derivatives being employed to provide multifunctional systems where the redox properties of ferrocene are coupled to other physical–chemical properties. Examples of this include new materials for non-linear optics, which have been obtained by associating ferrocene to oligomers, or biosensors which were obtained in conjunction with enzymes [4].

Ferrocene-1,1′-dicarboxylate (fdc^{2-}) possesses two additional features of interest for Mn chemistry: (i) it is a dicarboxylate with restricted flexibility and thus provides the possibility of obtaining Mn clusters not attainable with simple monocarboxylates; and (ii) it is readily introduced by reaction of the $fdcH_2$ form with a preformed Mn carboxylate cluster leading to incorporation of fdc^{2-} by the well-established carboxylate exchange process [5]. This attachment of the fdc^{2-} carboxylate groups directly onto the Mn atoms should allow coupling of a subsequent ferrocenium ($S = 1/2$) radical with the Mn/O magnetic core. In this paper, we describe the necessary first step of this project, the development of convenient methods to Mn_x clusters containing multiple fdc^{2-} ligands. In fact, we have prepared three structural types of nuclearities Mn_7, Mn_8 and Mn_{13}, each of which contain six fdc^{2-} groups attached to the metal core.

* Corresponding author. Tel.: +1 352 392 6737; fax: +1 352 392 8757.
E-mail address: christou@chem.ufl.edu (G. Christou).

0277-5387/$ - see front matter
doi:10.1016/j.poly.2006.11.014

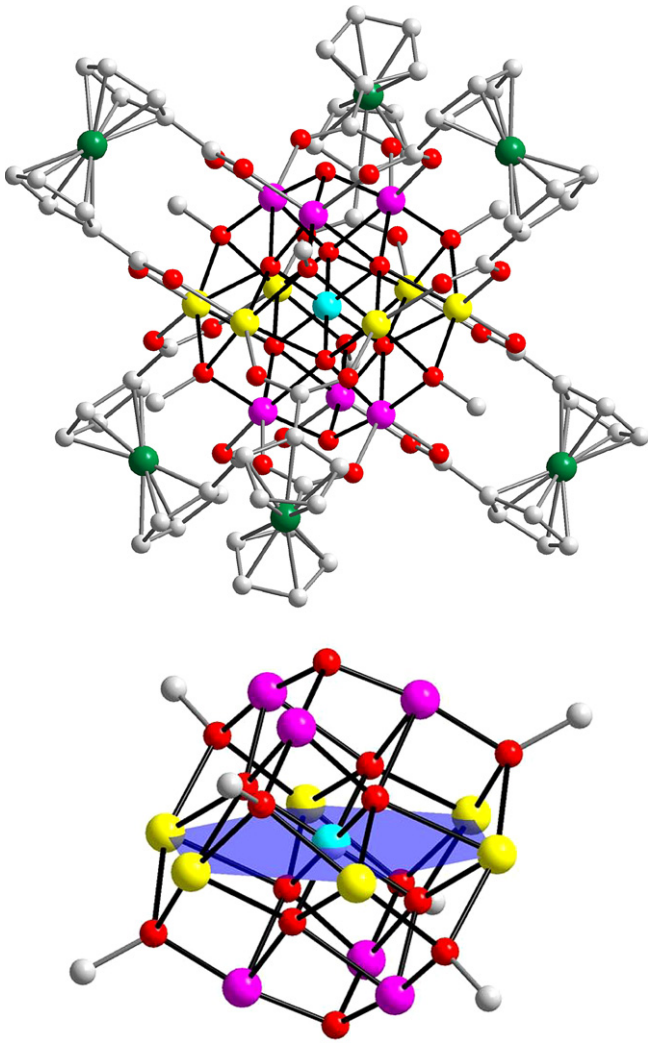

Fig. 1. Pov-Ray representation of **1** (top) and its core (bottom): Mn^{IV} (cyan), Mn^{III} (purple), Mn^{II} (yellow), O (red), Fe (green). Hydrogen atoms have been omitted for clarity. (For interpretation of the references to color in this figure legend, the reader is referred to the web version of this article.)

The reaction between $[Mn_{12}O_{12}(O_2CMe)_{16}(H_2O)_4]\cdot 2MeCOOH\cdot 4H_2O$ and $fdcH_2$ in a 1:4 molar ratio in CH_2Cl_2/MeOH (1:1) gave a dark brown suspension, which was filtered. The filtrate slowly forms dark brown needles of $[Mn_{13}O_8(OMe)_6(fdc)_6]\cdot 8CH_2Cl_2$ (**1** · $8CH_2Cl_2$) suitable for X-ray crystallography.[1] The same product resulted from reactions in different solvent mixtures such as MeCN/MeOH. The core can be described as consisting of three layers: there is a central layer comprising a Mn^{II}_6 hexagon with a central Mn^{IV} atom, and a Mn^{III}_3 triangular unit above and below this (Fig. 1). The core is held together by bridging O^{2-} and MeO^- groups, and the peripheral ligation is provided by six μ_4-fdc^{2-} groups. Complex **1** is a known compound, having been obtained previously by Horiba et al. using a different procedure [3], and the same Mn_{13} core has also been observed with benzoate ligation by Sun et al. [6]. We have also prepared the ethoxide analogue of **1** by repeating the reaction in CH_2Cl_2/EtOH, which gave $[Mn_{13}O_8(OEt)_6(fdc)_6]\cdot 7EtOH$ (**2** · 7EtOH). The complex was not structurally characterized by X-ray crystallography, but instead it was identified by the similarity of its IR spectrum and magnetic properties with those of **1**, and by its elemental analysis. The procedure to complex **2** is actually superior to that for **1** in that it gives a cleaner reaction and a higher yield of product. In particular, the crystallization solutions show no sign of minor side-products, as sometimes plagues the preparation of **1**.

The filtration residue from the reaction that gives **1** or **2** was treated with DMF resulting in a dark brown suspension. This was filtered and the filtrate left undisturbed to slowly yield dark brown needles of the novel complex $[Mn_8O_4(fdc)_6(DMF)_2(H_2O)_2]\cdot 4DMF\cdot 4H_2O$ (**3** · 4DMF · $4H_2O$) suitable for X-ray crystallography.[2] Complex **2** contains a core comprising a central $[Mn^{III}_4(\mu_4\text{-}O)_4]^{4+}$ cubane to each O^{2-} ion of which is attached a Mn^{II} atom (Fig. 2). The Mn_8 topology is thus two concentric Mn_4 tetrahedra. There are six fdc^{2-} groups, each carboxylate group of which bridges a Mn^{II}/Mn^{III} pair in the same *syn*, *syn* $\eta^1{:}\eta^1{:}\mu_2$-mode seen in **1**. The peripheral ligation is completed by a terminal DMF ligand on two of the Mn^{II} atoms, and a terminal H_2O ligand on the remaining two. As a result, the Mn^{III} and Mn^{II} atoms are six- and five-coordinate with near-octahedral and trigonal bipyramidal geometries, respectively. The metal oxidation states were again confirmed by charge considerations, bond valence sum (BVS) calculations [7,8], and the observation of Mn^{III} Jahn–Teller distortions. The torsion angles between the two carboxylate groups of the fdc^{2-} ligands vary: four fdc^{2-} groups have torsion angles of $<30°$ (synperiplanar configuration) and the other two have angles between 30° and 90° (synclinal configuration) [9].

Since $fdcH_2$ had given two interesting complexes from its reactions with $[Mn_{12}O_{12}(O_2CMe)_{16}(H_2O)_4]\cdot 2MeCOOH\cdot 4H_2O$, we also explored other reactions with various Mn^{II} starting materials. The reaction of $Mn(ClO_4)_2\cdot 6H_2O$ and $fdcH_2$ in a 1:1 molar ratio in DMF/MeOH (ratio 1:1) formed an orange suspension. This was filtered and the filtrate layered with Et_2O. Dark brown crystals of $[Mn_7O_3(OMe)(fdc)_6(H_2O)_3]\cdot 3DMF\cdot 3MeOH$ (**4** · 3DMF · 3MeOH) slowly grew as hexagonal plates that were suitable for X-ray crystallography.[3] The structure of **4** is somewhat

[1] *Crystal data for* **1** · $8CH_2Cl_2$: $C_{86}H_{82}Cl_{16}Mn_{13}Fe_6O_{38}$, $M_r = 3340.10$, triclinic, $P\bar{1}$, $a = 14.1308(12)$ Å, $b = 15.1738(12)$ Å, $c = 15.3656(13)$ Å, $\alpha = 119.4700(10)°$, $\beta = 91.4320(10)°$, $\gamma = 100.339(2)°$, $V = 2797.0(4)$ Å^3, $Z = 1$, $T = 173(2)$ K, $R_1 = 0.0479$, $wR_2 = 0.1190$ (F^2 all data), 18 432 reflections.

[2] *Crystal data for* **3** · 4DMF · $4H_2O$: $C_{90}H_{102}N_6Mn_8Fe_6O_{40}$, $M_r = 2682.40$, monoclinic, $C2/c$, $a = 23.282(3)$, $b = 19.331(3)$, $c = 22.198(3)$ Å, $\alpha = 90°$, $\beta = 97.885(3)°$, $\gamma = 90°$, $V = 9896(3)$ Å^3, $Z = 4$, $T = 173(2)$ K, $R_1 = 0.0934$, $wR_2 = 0.1117$ (F^2 all data), 32 126 reflections.

[3] *Crystal data for* **4** · 6MeOH: $C_{85}H_{90}N_3Mn_7Fe_6O_{37}$, $M_r = 2465.30$, rhombohedral, $R3$, $a = 15.8534(6)$, $b = 15.8534(6)$, $c = 64.090(5)$ Å, $\alpha = 90°$, $\beta = 90°$, $\gamma = 120°$, $V = 13949(13)$ Å^3, $Z = 6$, $T = 173(2)$ K, $R_1 = 0.0566$, $wR_2 = 0.1016$ (F^2 all data), 21 258 reflections.

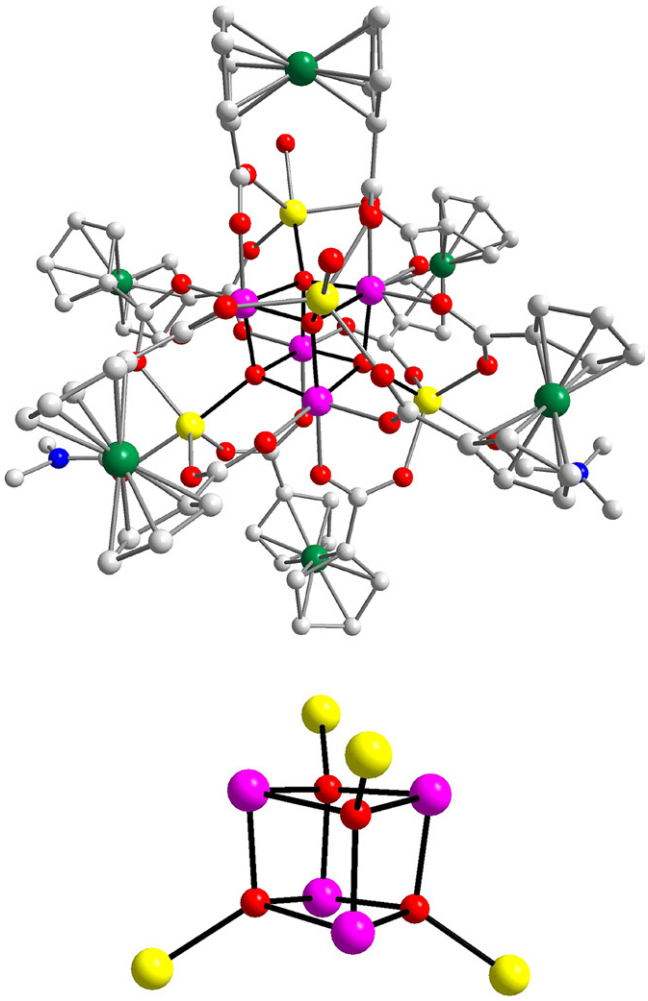

Fig. 2. Pov-Ray representation of **3** (top) and its core (bottom): Mn^{III} (purple), Mn^{II} (yellow), O (red), N (blue), Fe (green). Hydrogen atoms have been omitted for clarity. (For interpretation of the references to color in this figure legend, the reader is referred to the web version of this article.)

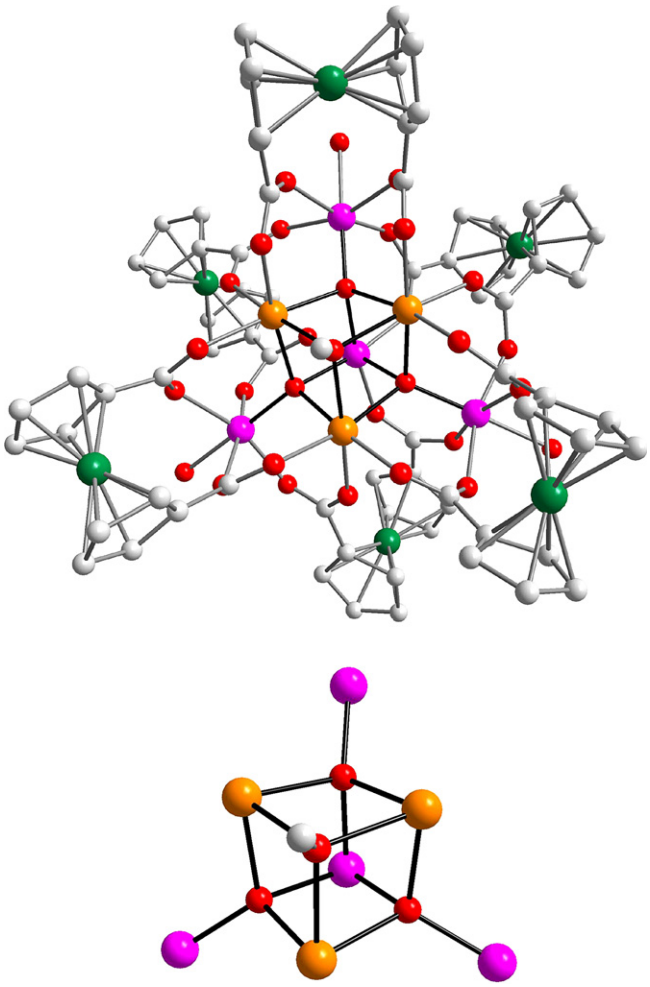

Fig. 3. Pov-Ray representation of complex **4** (top) and its core (bottom). Mn^{III} (purple), disordered $2Mn^{II}$ plus Mn^{III} (orange), O (red), Fe (green). Hydrogen atoms have been omitted for clarity. (For interpretation of the references to color in this figure legend, the reader is referred to the web version of this article.)

similar to that of **3** in that there is a central Mn_4O_4 cubane, but one of the O atoms is now part of a MeO^- group, rather than an O^{2-} ion, and thus there are only a total of three additional Mn atoms, each attached to one of the three O^{2-} ions of the central cubane (Fig. 3). The overall $[Mn_7(\mu_4\text{-}O)_3(\mu_3\text{-}OMe)]$ core is unprecedented.

The Mn oxidation states of **4** are not analogous to those in **3**, and this represents another major difference between the two structures. The oxidation states have been probed by BVS calculations, and the results were overall consistent with charge balance considerations based on the electroneutrality of the complex, and assuming none of the ferrocene groups are in the oxidized form, but with a few uncertainties in the precise details. The following preliminary conclusions have been reached: the three exterior Mn atoms attached to the cubane are all clearly Mn^{III}. The three Mn atoms in the central cubane core bridged by the MeO^- group are related by the crystallographic C_3-axis and thus give the same BVS value, which is characteristic of an average oxidation state less than 2.5+. We thus conclude that these three Mn atoms comprise one Mn^{III} and two Mn^{II} that are statically disordered by the symmetry axis. In other words, their Mn–O bond lengths are in-between those typical for true Mn^{III}–O and Mn^{II}–O bonds. The remaining Mn atom in the cubane and diagonally opposite the MeO^- group (Fig. 3) was expected, on the basis of charge neutrality, to be Mn^{III} but had a BVS lower than expected, and we believe this may be due to a Mn^{III}/ferrocene versus Mn^{II}/ferrocenium static disorder, i.e. one of the ferrocenes may be oxidized. At this time, we cannot unequivocally conclude anything more definite, but this point is currently under further investigation and will be discussed in more detail in the full paper.

There are again six fdc^{2-} groups providing the peripheral ligation about the core, which can be divided into two sets with equivalent torsion angles and binding modes within each set. In fact, this is the first case in this work where we have seen the fdc^{2-} groups to adopt different binding conformations, and no doubt this is due to the

lower symmetry of **4** compared to **1** and **3**. The three Mn^{III} atoms outside the cubane define a plane that divides the two sets of fdc^{2-} groups; the set lying on the opposite to the methoxide has the same kind of binding mode as in **1** and **3**, i.e. each fdc^{2-} attaches to a total of four Mn atoms in an $\eta^1{:}\eta^1{:}\eta^1{:}\eta^1{:}\mu_4$ bridging mode with a torsion angle of 6.48°. In contrast, the other set of fdc^{2-} groups bind to a total of three Mn atoms in an $\eta^1{:}\eta^1{:}\eta^1{:}\eta^1{:}\mu_3$-mode with a torsion angle of 26.67°. Thus, each carboxylate O atom is still attached to only a single Mn atom, but two of them are now attached to the same Mn^{III} atom, the one external to the cubane. Finally, there is a terminal H_2O group bound to each external Mn^{III} atom, and all Mn atoms are consequently six-coordinate with near-octahedral geometries.

Magnetic susceptibility (χ_M) data were collected for complexes **1**–**4** on polycrystalline samples in a 0.1 T DC field in the 5.00–300.00 K temperature range. The data for **1** and **2** were essentially superimposable, and thus we report here only the data for complexes **2**, **3** and **4** (Fig. 4). $\chi_M T$ for **2** is almost constant at ~47 cm^3 K mol^{-1} from 300 to 150 K and then decreases steadily to 11.54 cm^3 K mol^{-1} at 5.00 K. This suggests the presence of dominant antiferromagnetic exchange interactions within the cluster. $\chi_M T$ for **3** remains almost constant with decreasing temperature, with a value close to ~15 cm^3 K mol^{-1} for the entire temperature range. It fluctuates with decreasing temperature before reaching a value of 13.64 cm^3 K mol^{-1} at 5.00 K. $\chi_M T$ for **4** decreases steadily from 12.00 cm^3 K mol^{-1} at 300 K to 2.43 cm^3 K mol^{-1} at 5.00 K, again indicating dominant antiferromagnetic interactions within the molecule.

Complexes **2**, **3** and **4** are too large and/or too low symmetry for easy determination of the various pairwise exchange parameters J_{ij} between two Mn atoms Mn_i and Mn_j, and we therefore concentrated instead on determining their ground state spin (S) values. This was carried out by two independent methods, fitting of their variable-temperature (T) and -field (H) DC magnetization data, and AC susceptibility measurements. DC magnetization (M) data were collected in the 1.8–10.0 K range in fields varying between 0.1 and 7 T, and fit to a model that assumes only the ground state is populated, includes axial zero-field splitting ($\widehat{S}_z^2 D$) and the Zeeman interaction ($g\mu_B\mu_0\widehat{S}\cdot H$), and incorporates a full powder average. The obtained best-fit S, g and D values for complexes **2**–**4** are listed in Table 1. In order to avoid complications from low-lying excited states, data collected in very high DC fields were not employed. For **2** and **4**, we could only get good fits by using data collected only in fields up to 0.8 T. For **3**, data up to higher field values could be employed.

The ground state S values for **2**–**4** were confirmed by AC susceptibility measurements in the temperature range 1.8–15 K using a 3.5 G AC field oscillating at a frequency of 50, 250 and 997 Hz. AC susceptibility studies are performed in the absence of a DC field and therefore avoid the problems caused by low-lying excited states. The real, or in-phase, AC susceptibility (χ'_M) of complexes **2**–**4** is plotted as $\chi'_M T$ versus T in Fig. 5. Extrapolation of the plots to 0 K, from temperatures above ~4 K to avoid the effects of weak intermolecular interactions (dipolar and superexchange), gives values of ~11, ~13 and ~2.5 cm^3

Table 1
The g and D values obtained from fits of magnetization data for complexes **2**–**4**

Complex	Fields (T)	S	g[a]	D (cm^{-1})[b]
2	0.1–0.8	9/2	1.91	−0.23
3	0.1–4	5	1.97	−0.32
4	0.1–0.8	2	1.81	−0.93

[a] ±0.01.
[b] ±0.05 cm^{-1}.

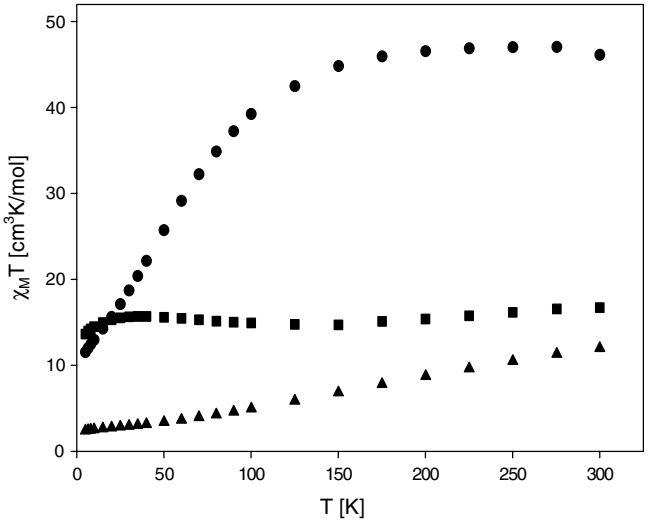

Fig. 4. Plot of $\chi_M T$ vs. T for complexes **2** (●), **3** (■) and **4** (▲).

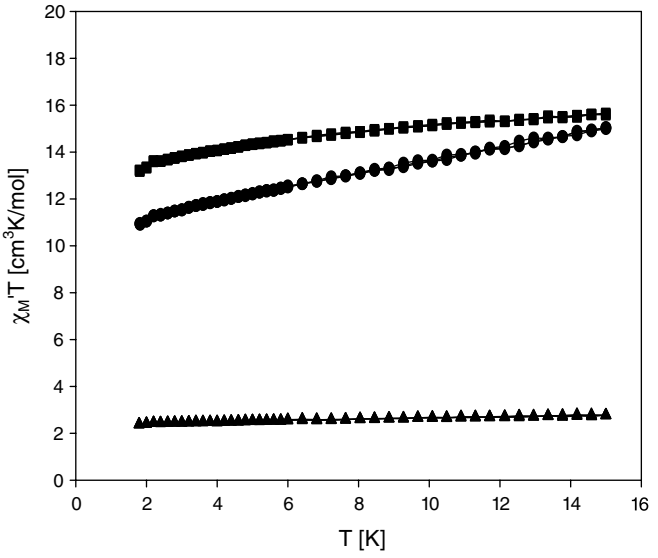

Fig. 5. Plot of $\chi'_M T$ vs. T for complexes **2** (●), **3** (■) and **4** (▲); the signals at 50, 250 and 997 Hz are essentially superimposed.

K mol^{-1}, confirming ground state S values of 9/2, 5 and 2, respectively (with $g < 2$, as expected for Mn), in satisfying agreement with the DC magnetization fits. None of the complexes displayed out-of-phase (χ''_M) AC susceptibility peaks above 1.8 K, the operating limit of our SQUID magnetometer. There were some signs of the beginnings of signals whose peaks lie below 1.8 K, and these may correspond to the very small dips in the $\chi'_M T$ plots of Fig. 5 at $T < 2$ K. Studies at temperatures below 1.8 K are in progress to explore this point further.

In summary, the use of $fdcH_2$ in Mn cluster chemistry has led to an interesting family of ferrocene-rich Mn_7, Mn_8 and Mn_{13} complexes. The latter two were obtained by a carboxylate substitution reaction on $[Mn_{12}O_{12}(O_2CMe)_{16}(H_2O)_4] \cdot 2MeCOOH \cdot 4H_2O$, which caused structural changes to the core. Although the core of Mn_{13} has been seen before, the present work has provided both a convenient synthetic route and also a means to prepare the previously unknown ethoxide analogue. All three structural types possess non-zero ground state spin values, although they do not seem to be new examples of single-molecule magnets, at least based on data collected at >1.8 K. The described work represents the desired synthetic breakthrough into this area of ferrocene-rich Mn clusters, and work is currently in progress to investigate the electrochemical properties of these clusters. Indeed, preliminary results on **4**, the easiest to study because of its high solubility, show rich redox behavior with multiple reversible processes.

Acknowledgement

We thank the National Science Foundation for supporting this work.

Appendix A. Supplementary material

CCDC 622659, 622660 and 622661 contain the supplementary crystallographic data for this paper. These data can be obtained free of charge via http://www.ccdc.cam.ac.uk/conts/retrieving.html, or from the Cambridge Crystallographic Data Centre, 12 Union Road, Cambridge CB2 1EZ, UK; fax: (+44) 1223-336-033; or e-mail: deposit@ccdc.cam.ac.uk. Supplementary data associated with this article can be found, in the online version, at doi:10.1016/j.poly.2006.11.014.

References

[1] (a) D.M. Kurtz, Chem. Rev. 90 (1990) 585;
(b) E.J.M. Hensen, J.A.R. van Veen, Catal. Today 86 (2003) 87.
[2] (a) For reviews, see: G. Christou, D. Gatteschi, D.N. Hendrickson, R. Sessoli, MRS Bull. 25 (2000) 66;
(b) G. Aromi, E.K. Brechin, Struct. Bond. 122 (2006) 1;
(c) R. Bircher, G. Chaboussant, C. Dobe, H.U. Güdel, S.T. Oshsenbein, A. Sieber, O. Waldmann, Adv. Funct. Mater. 16 (2006) 209;
(d) D. Gatteschi, R. Sessoli, Angew. Chem., Int. Ed. 42 (2003) 268.
[3] M. Kondo, R. Shinagawa, M. Miyazawa, M. Kabir, Y. Irie, T. Horiba, T. Naito, K. Maeda, S. Utsuno, F. Uchida, Dalton Trans. (2003) 515.
[4] (a) J.A. Mata, E. Peris, R. Llusar, S. Uriel, M.P. Cifuentes, M.G. Humphrey, M. Samoc, B. Luter-Davies, Eur. J. Inorg. Chem. (2001) 2113;
(b) U. Löffler, W. Göpel, B. Speiser, Electroanalysis 3 (9) (1991) 917.
[5] M. Soler, W. Wernsdorfer, K.A. Abboud, J.C. Huffman, E.R. Davidson, D.N. Hendrickson, G. Christou, J. Am. Chem. Soc. 135 (2003) 3576.
[6] Z. Sun, P. Gantzel, D. Hendrickson, Inorg. Chem. 35 (1996) 6640.
[7] I.D. Brown, D. Altermatt, Acta Crystallogr. B41 (1985) 244.
[8] W. Liu, H.H. Thorp, Inorg. Chem. 32 (1993) 4102.
[9] IUPAC, Compendium of Chemical Terminology, 2nd ed., 1997.